

DISTORTION OF MAGNETIC AND ELECTRICAL FIELDS BY NEAR-SURFACE LATERAL INHOMOGENEITIES

M. N. BERDICHEVSKIY—V. I. DMITRIEV

MOSCOW STATE UNIVERSITY
FACULTY OF GEOLOGY AND COMPUTING CENTRE, MOSCOW, USSR

The authors consider the general interpretation strategy which takes into account the surface effects and present some results obtained in this field in the U.S.S.R. The paper consists of five sections discussing the following questions: *a)* strategy for interpretation of magnetotelluric and magnetovariation data, *b)* simulation of surface effects, *c)* theoretical analysis of these effects, *d)* their diagnostics and *e)* elimination of field distortion.

Introduction

Geophysicists, when they began the first deep geological investigations, could hardly imagine that the distortion of electromagnetic field by the near-surface inhomogeneities would give rise to serious difficulties. The optimism which prevailed in the early fifties can be clearly perceived in the paper of CAGNIARD [11]. But as years passed by, it has become evident that the near-surface layer formed by the sediments of continents and oceanic waters might significantly distort the electromagnetic field studied by magnetotelluric or magnetovariation methods. Magnetotelluric sounding carried out at different regions of the globe demonstrated a great deal of such distortions. Many geomagnetic anomalies detected in Europe and in Asia by magnetovariation method were found to be rather of surface than deep origin. All these facts compelled the geophysicists to reject the naive interpretation and to search for methods that would account for the surface effects. The rapid advance of this work was due to the mathematical and physical simulation of horizontally inhomogeneous media. Many aspects of this problem have already been reviewed in Edinburgh (1972) and in Ottawa (1974). In this review, therefore, we shall confine ourselves to a consideration of the general interpretation strategy which accounts for the surface effects, and presents some recent results obtained in this field in the U.S.S.R.

1. Strategy for the interpretation of magnetotelluric and magnetovariation data

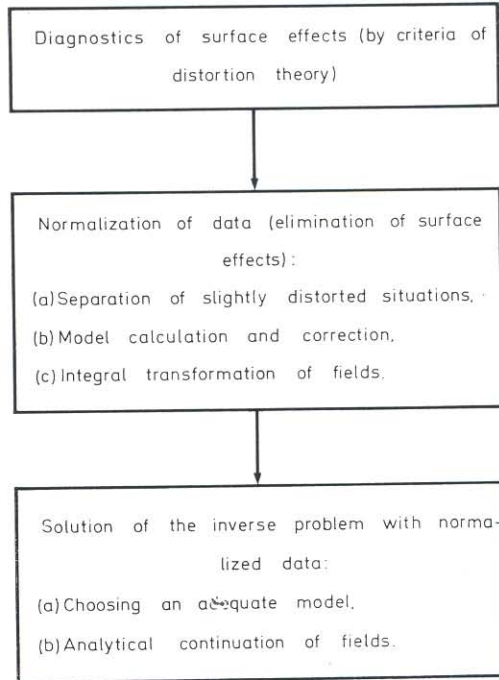
Had the surface effects been weak, interpretation could have been directly reduced to the solution of the inverse problem, i.e. the determination of distribution of deep electrical conductivity. Such a simple approach, unfortunately, often leads to profound errors caused by the surface effects. The MTS curves are deformed and their formal interpretation using horizontally homogeneous models gives rise to false geoelectrical structures. Similarly, a false picture is obtained from magnetovariation data if the surface anomalies are regarded as deep ones. Interpretation gets more complicated if the surface effects are taken into consideration. Prior to solving the inverse problem, it is essential to eliminate the field distortions created by near-surface inhomogeneities. If the structure of the near-surface layer is known, then it is possible to eliminate the influence of its inhomogeneity with the help of an integral transformation of the field. In this approach, however, a considerable amount of local information is lost; moreover, errors creep in because of the inadequacy of the model. It would, therefore, be advantageous to combine integral field transformations with preliminary diagnostics of the surface effects. This allows us to estimate the degree of the influence of surface effects, to substantiate the choice of the model, and to obtain fuller local information. Consequently, it would be natural to interpret the magnetotelluric and magnetovariation data according to a three-stage scheme (Table 1):

- diagnostics of surface effects,
- normalization of data, i.e. elimination of surface effects,
- solution of the inverse problem with normalized data, i.e. determination of the distribution of deep electrical conductivity.

These three stages are so closely interconnected that they can be isolated only conditionally.

The main problem in the first stage is to detect and typify the surface effects. It calls for a special theory studying surface effects in typical geological situations. Such a theory based on the simplest models of inhomogeneous media exposes the nature of surface effects and gives methods for recognizing and classifying these effects. Success in the practical application of such methods largely depends on the amount of experimental data available. The results derived are mainly qualitative, nevertheless, they can be refined by approaching the models to actual geological situations. This stage should give a clear idea of the morphology of surface effects and the degree of their influence. Some geophysicists prefer to choose straightway complex models which approximate the real situation. Such an approach, however, does not seem to be very fruitful as it is hard to obtain a satisfactory agreement between calculations and experiments without preliminary typification of surface effects.

Table I
THE SCHEME FOR INTERPRETATION OF MAGNETOTELLURIC
AND MAGNETOVARIAION DATA



The second stage consists in eliminating the field distortions. Three different techniques can be recommended for this purpose. The first is based on the use of criteria of distortion theory and on the separation of slightly distorted situations. Such an approach is very effective in interpreting the magnetotelluric data for obtaining local information. The second is connected with the simulation of real situations and introduction of corrections into magnetotelluric and magnetovariation data. The third uses integral transformations of fields, this is a very attractive technique as it readily yields to formulization and gives a universal solution to the problem. In the subsequent pages we shall demonstrate that the spatial Fourier field analysis permits to obtain electromagnetic sounding curves which are free from the effect of near-surface inhomogeneities, and to divide the variable geomagnetic field anomalies into surface and deep parts. We have already mentioned the drawbacks of this approach. Each technique supplements the other. The success of interpretation as a whole largely depends on the extent to which the surface effects are eliminated.

Interpretation ends in the third stage which consists in the determination

of deep electrical conductivity. The inverse problem is solved by choosing an adequate model. Of late, efforts are being diverted towards developing methods based on analytical continuation of fields. This interesting topic, however, is beyond the scope of our review.

2. Simulation of surface effects

We shall examine three main points of this problem:

1. selection of models for the external field;
2. selection of models for the Earth;
3. methods for studying the models.

External field models

The models should approximate the most significant part of the external electromagnetic field of the Earth. It is known that this field has E -toroidal and H -toroidal modes. The contribution of the H -toroidal mode to the tangential components of the total field has been repeatedly considered in literature [25, 43, 53, 4, 21]. This contribution has been shown to be negligibly small, at least, in the frequency range used for the determination of the Earth's electrical conductivity. Consequently, we have to examine only the induction action of the external field represented by the E -toroidal mode. To approximate this field it is sufficient to take a few active harmonics of its spatial spectrum. Best approximation is obtained in the simulation of world magnetic storms and diurnal solar variations for which the spatial spectra have been investigated in great detail. Spatial spectra of pulsations and bays have so far not been studied to that extent. The configuration of external fields of these variations are highly changeable. They can, however, be considered in a limited domain, and thus the Earth's sphericity could be disregarded and the external field approximated by a non-uniform plane wave [49]. If the domain under consideration is sufficiently small, the external field can be represented as a uniform plane wave. This simple and convenient model is known as the TIKHONOV—CAGNIARD model [11, 45, 46]. The feasibility of such an approximation has been disputed for long [36, 50, 30, 42, 37, 47]. This prolonged discussion, indeed, was very fruitful as it determined the limits of applicability of the TIKHONOV—CAGNIARD model. These limits proved to be so wide that uniform plane waves began to be used for simulating the local conductive anomalies in world magnetic storms and in solar diurnal variations.

Thus, the models for the external field have to be chosen with respect to the type of variations and the scale of near-surface inhomogeneity. Local effects are satisfactorily simulated by the TIKHONOV—CAGNIARD model.

Models of the Earth

In order to develop a distortion theory, we need a series of models that would describe the behaviour of the electromagnetic field in typical geological situations. Such models have cognitive value. They consist of a near-surface layer containing elementary structures, and uniform layers for describing the Earth's crust and upper mantle. The three-layer model of the type "non-uniform near-surface layer — uniform intermediate layer of higher resistivity — perfectly conducting basement" is considered as fundamental. Structures for the near-surface layer are chosen depending on the type of effects to be studied. The model of semispherical ocean [1, 37] is an example of global structure. Structures of the type "horst", "graben", "inclined contact", etc. simulate the local effects [18, 27, 34, 10].

Investigation of models

The mathematical and physical models are used for studying the near-surface effects. Mathematical modelling has been rapidly developed in the last decade. Today, the following methods are applied in geoelectrical investigations: finite-difference method, method of finite elements, projection method, integral equation method, and asymptotic method. A wide class of two-dimensional problems has been thoroughly investigated, and the first three-dimensional problems are being solved at present. Physical models, mostly three-dimensional ones, are being investigated using liquid and solid media. The difference methods and physical simulation methods have been reviewed in detail by JONES [28], PRAUS [34], DOSSO [23] and WARD [51]. Integral equation, projection and asymptotic methods have been treated less extensively and precisely these are the methods we shall deal with in this review.

Integral equation method

This method is very convenient for calculating simple two-dimensional models which form the basis of distortion theory. We shall examine two approaches for deriving the integral equations.

In the classical approach the two-dimensional boundary value problem is reduced to an integral equation on the transverse section of inhomogeneity [29, 13, 51]. Let us consider a three-layer model in which the near-surface layer contains a cylindrical inhomogeneity bounded by a contour C . The geometry of the model and its parameters are shown in Fig. 1. The magnetic permeability is equal to μ_0 everywhere. The contour C divides the plane yz into an outer region ($Q^e = Q_0$ (air) + Q_1^e (near-surface layer) + Q_2 (intermediate layer) + Q_3 (perfect conductor)) and an inner region Q_1^i (inhomogeneity). The

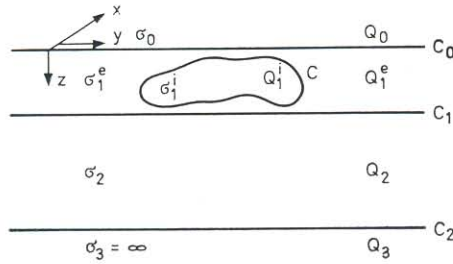


Fig. 1. Two-dimensional model with horizontal cylindrical inhomogeneity

boundaries of the layers are C_0 , C_1 and C_2 . The sources of the E - or H -polarized field are distributed in Q_0 . The electromagnetic field can be described by the function:

$$F(M) = \begin{cases} E_x(M) & E\text{-polarization} \\ H_x(M) & H\text{-polarization.} \end{cases}$$

In the quasi-stationary approximation F satisfies the following equation:

$$\mathcal{H}[F(M)] = \begin{cases} I(M) & M \in Q_0 \\ 0 & M \in Q_1 + Q_2. \end{cases}$$

where I is the source density, \mathcal{H} is the Helmholtz operator:

$$\mathcal{H} = \begin{cases} \mathcal{H}_m^e = \Delta + i\omega\mu_0\sigma_m & M \in Q_m \ (m = 0, 2) \\ \mathcal{H}_1^e = \Delta + i\omega\mu_0\sigma_1^e & M \in Q_1^e \\ \mathcal{H}_1^i = \Delta + i\omega\mu_0\sigma_1^i & M \in Q_1^i. \end{cases}$$

The functions F and $1/p \cdot \partial F / \partial n$ are continuous on the contour C and on the boundaries C_0 , C_1 (n is the normal to the line of discontinuity of σ and $p = 1$ for E -polarization or $p = \sigma$ for H -polarization). On the boundary C_2 the function F satisfies the condition $F=0$ (E -polarization) or $\partial F / \partial z=0$ (H -polarization).

We shall introduce the outer Green function G^e defined by the equation:

$$\mathcal{H}_m^e[G^e(M, M')] = -\delta(r_{MM'})$$

$$M' \in Q_1 \quad M \in Q_0 + Q_1 + Q_2 \quad m = 0, 1, 2.$$

On the boundaries C_0 and C_1 the functions G^e and $1/p(\partial G^e / \partial z)$ are continuous, and on the boundary C_2 the function G^e satisfies the condition $G^e = 0$ (E -polarization) or $\partial G^e / \partial z = 0$ (H -polarization).

Applying the Green theorem to the regions Q_1^i and Q^e , we obtain

$$\begin{aligned} & i\omega\mu_0(\sigma_1^i - \sigma_1^e) \iint_{Q_1^i} F^i(M') G^e(M, M') dq_{M'} - \\ & - \oint_C \left[F^i(M') \frac{\partial G^e(M, M')}{\partial n_{M'}} - G^e(M, M') \frac{\partial F^i(M')}{\partial n_{M'}} \right] dl_{M'} = \quad (1) \\ & = \begin{cases} F^i(M) & M \in Q_1^i \\ 0 & M \in Q^e \end{cases} \end{aligned}$$

$$\begin{aligned} F^N(M) + \oint_C \left[F^e(M') \frac{\partial G^e(M, M')}{\partial n_{M'}} - G^e(M, M') \frac{\partial F^e(M')}{\partial n_{M'}} \right] dl_{M'} = \\ = \begin{cases} 0 & M \in Q_1^i \\ F^e(M) & M \in Q^e \end{cases}, \quad (2) \end{aligned}$$

where F^i and F^e are the fields in the inner and outer regions of the near-surface layer and their limiting values on the contour C , F^N is the normal field in the near-surface layer.

Multiplying the first and second equations by $1/p_1^i$ and $1/p_1^e$ respectively, and adding them, we obtain by virtue of the boundary conditions on C a Fredholm integral equation of the second kind for the inner field:

$$\begin{aligned} F^i(M) + i\omega\mu_0(\sigma_1^e - \sigma_1^i) \iint_{Q_1^i} F^i(M') G^e(M, M') dq_{M'} + \\ + \left(1 - \frac{p_1^i}{p_1^e} \right) \oint_C F^i(M') \frac{\partial G^e(M, M')}{\partial n_{M'}} dl_{M'} = \frac{p_1^i}{p_1^e} F^N(M), \\ M \in Q_1^i \quad (3) \end{aligned}$$

and an integral representation for the outer field in terms of the inner field:

$$\begin{aligned} F^e(M) = F^N(M) + i\omega\mu_0 \frac{p_1^e}{p_1^i} (\sigma_1^i - \sigma_1^e) \iint_{Q_1^i} F^i(M') G^e(M, M') dq_{M'} + \\ + \left(1 - \frac{p_1^e}{p_1^i} \right) \oint_C F^i(M') \frac{\partial G^e(M, M')}{\partial n_{M'}} dl_{M'}, \quad M \in Q^e. \quad (4) \end{aligned}$$

For calculating the field, a network is used to reduce the integral equation to a system of algebraic equations. If the dimension of inhomogeneity is not large, only a small number of cells is needed for studying a low-frequency field and the calculations can be carried out at a sufficiently rapid rate. In such cases it is quite possible to save calculation time as compared with the difference method.

The time gain is much more appreciable in the second approach in which a two-dimensional boundary value problem is reduced to a system of integral equations on the inhomogeneity contour [31, 15]. We introduce an inner Green function which in the entire space satisfies the following equation:

$$\mathfrak{H}_1^i[G^i(M, M')] = -\delta(r_{MM'}).$$

On applying the Green theorem to the region Q_1^i we obtain

$$\oint_C \left[F^i(M') \frac{\partial G^i(M, M')}{\partial n_{M'}} - G^i(M, M') \frac{\partial F^i(M')}{\partial n_{M'}} \right] dl_{M'} = 0, \quad M \in Q_1^e.$$

Adding this result to equation (2), by virtue of the conditions on the contour C , we find that

$$F^e(M) = F^N(M) + \oint_C \left\{ F^e(M') \frac{\partial [G^e(M, M') - G^i(M, M')]}{\partial n_{M'}} - \left[G^e(M, M') - \frac{p_1^i}{p_1^e} G^i(M, M') \right] \frac{\partial F^e(M')}{\partial n_{M'}} \right\} dl_{M'}, \quad M \in Q_1^e. \quad (5)$$

Such an integral representation permits the determination of the field at any point in the region Q_1^e using the limiting values of F^e and $\partial F^e/\partial n$ given on the contour C . These values are found from the system of integral equations. To derive the first equation, we shall take the point M on the contour C :

$$F^e(M) - \oint_C \left\{ F^e(M') \frac{\partial [G^e(M, M') - G^i(M, M')]}{\partial n_{M'}} - \left[G^e(M, M') - \frac{p_1^i}{p_1^e} G^i(M, M') \right] \frac{\partial F^e(M')}{\partial n_{M'}} \right\} dl_{M'} = F^N(M), \quad M \in C. \quad (6)$$

The second equation can be obtained by differentiating (5) along the normal to the contour C . The integral in (5) contains the difference in the potentials of simple layers with densities $\nu = \partial F^e/\partial n$ and $\nu = (p_1^i/p_1^e)(\partial F^e/\partial n)$. The outer limiting value of the normal derivative of the potential of a simple layer is given by

$$\frac{\partial}{\partial n_M} \oint_C \nu(M') G(M, M') dl_{M'} = \oint_C \nu(M') \frac{\partial G(M, M')}{\partial n_M} dl_{M'} - \frac{1}{2} \nu(M), \quad M \in C.$$

Consequently, we have

$$\frac{1}{2} \left(1 + \frac{p_1^i}{p_1^e} \right) \frac{\partial F^e(M)}{\partial n_M} - \oint_C \left\{ F^e(M') \frac{\partial^2 [G^e(M, M') - G^i(M, M')]}{\partial n_M \partial n_{M'}} - \frac{\partial [G^e(M, M') - (p_1^i/p_1^e) G^i(M, M')]}{\partial n_M} \frac{\partial F^e(M')}{\partial n_{M'}} \right\} dl_{M'} = \frac{\partial F^N(M)}{\partial n_M}, \quad M \in C. \quad (7)$$

Thus, we obtain a system of Fredholm integral equations (6) and (7) of the second kind. This method is better than that suggested by PARRY [33] in which the boundary value problem is reduced to a system of integro-differential equations of the first kind.

A wide class of two-dimensional models were studied by these methods at the Moscow State University. Most instructive models are listed in Table II. Special albums have been published containing the theoretical curves characterizing various surface effects.

The integral equation method could be successfully applied for solving three-dimensional problems of axisymmetric inhomogeneity. Examples of such cases have been published by DMITRIEV et al. [17] and TABOROVSKIY [44]. The possibilities of the method for solving general three-dimensional problems have recently been demonstrated by WEIDELT [52].

Projection methods

These methods are very effective for studying the H -polarized field [12, 22]. We take up the model shown in Fig. 1 and assume that $\sigma_0 = 0$ and σ_1 is a continuous function of y, z . The magnetic field H_x satisfies the homogeneous equation:

$$\mathfrak{H}^*[H_x(M)] = \operatorname{div} \left[\frac{\operatorname{grad} H_x(M)}{\sigma(M)} \right] + i\omega\mu_0 H_x(M) = 0, \quad M \in Q_1 + Q_2 \quad (8)$$

and the inhomogeneous boundary conditions

$$\begin{aligned} H_x|_{C_0} = H_0 = \text{const} & \quad H_x^{(1)}|_{C_1} = H_x^{(2)}|_{C_1} \\ \frac{\partial H_x}{\partial z} \Big|_{C_2} = 0 & \quad \frac{1}{\sigma_1} \frac{\partial H_x^{(1)}}{\partial z} \Big|_{C_1} = \frac{1}{\sigma_2} \frac{\partial H_x^{(2)}}{\partial z}, \end{aligned} \quad (9)$$

where H_0 is doubled external field.

For solving this interior problem, we introduce the function $U = H_x - \tilde{H}$, where \tilde{H} is a known function satisfying the same boundary conditions (9). This function U evidently satisfies the inhomogeneous equation:

$$\mathfrak{H}^*[U(M)] = f(M) \quad M \in Q_1 + Q_2 \quad (10)$$

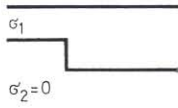
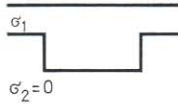
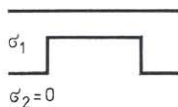

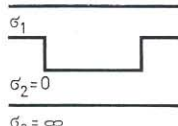
and the homogeneous boundary conditions

$$\begin{aligned} U|_{C_0} = 0 & \quad \frac{\partial U}{\partial z} \Big|_{C_2} = 0 & \quad U^{(1)}|_{C_1} = U^{(2)}|_{C_1}, \\ \frac{1}{\sigma_1} \frac{\partial U^{(1)}}{\partial z} \Big|_{C_1} & = \frac{1}{\sigma_2} \frac{\partial U^{(2)}}{\partial z} \Big|_{C_1}, \end{aligned} \quad (11)$$

where $f = -\mathfrak{H}^*[\tilde{H}]$.

Table II.

TWO-DIMENSIONAL MODELS STUDIED AT THE MOSCOW STATE UNIVERSITY
(Results published in the Album of MTS curves for horizontally non-uniform media)

Author	Model	Method	Polarization of field	Ref
1	2	3	4	5
Dmitriev, Kokotushkin		Projection method	H-polarization	Album, 1971
Dmitriev, Kokotushkin		Projection method	H-polarization	Album, 1971
Dmitriev, Kokotushkin		Projection method	H-polarization	Album, 1971
Dmitriev, Kokotushkin		Projection method	H-polarization	Album, 1971
Dmitriev, Kokotushkin		Integral equation method	E-polarization	Album, 1971

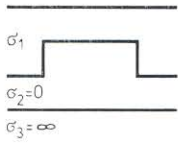
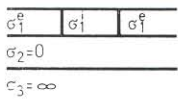
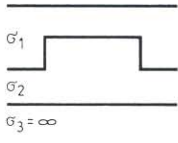
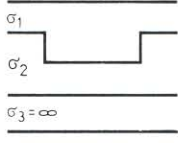
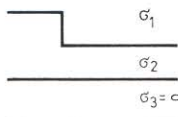
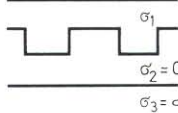
To find U we shall make use of the approximate representation:

$$U(M) \approx \tilde{U}(M) = \sum_{n=1}^N \tilde{U}_n(y) \varphi_n(z),$$

where $\{\varphi_n\}$ is some basic orthogonal system of functions satisfying the boundary conditions (11), and \tilde{U}_n is the projection of the function \tilde{U} . From the condition, $\min \|\mathcal{H}^*[\tilde{U}] - f\|_{L_2}$, which gives the best approximation, we obtain a system of ordinary differential equations for \tilde{U}_n . This system is easily solved by numerical methods.

A simplified modification is called the method of transverse sections. In this method, a model is divided into regions approximated by horizontally layered structures. In each region, the solution of the differential equation for \tilde{U}_n contains two unknown constants. These constants are determined from

Cont. of table II.

1	2	3	4	5
Dmitriev Kokotushkin		Integral equation method	E-polari- zation	Album, 1 1971
Zakharov		Integral equation method	E-polari- zation	Album, 2 1972
Dmitriev Kokotushkin		Integral equation method	H-polari- zation	Album, 2 1972
Dmitriev Kokotushkin		Integral equation method	H-polari- zation	Album, 2 1972
Dmitriev Kokotushkin		Integral equation method	H-polari- zation	Album, 2 1972
Dmitriev Kokotushkin		Integral equation method	E-polari- zation	Album, 3 1975

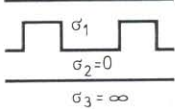
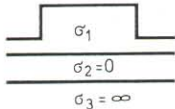
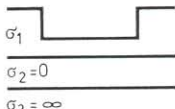
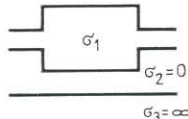
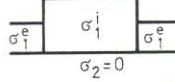
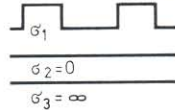
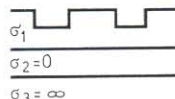
a system of algebraic equations derived from the conjugation conditions at the boundaries of the regions (these conditions hold true on the average). The method can be easily extended to models in which the near-surface layer has conductivity discontinuities.

The models calculated at the Moscow State University with the help of projection methods are listed in Table II.

Asymptotic methods

In many deep geoelectric problems we may confine ourselves to a study of the low-frequency asymptotics of the field. This simplifies the mathematical technique. Asymptotic methods have two distinct advantages: 1. they diminish the dimensionality of the problem, i.e. reduce a two-dimensional problem to

Cont. of table II.

1	2	3	4	5
Dmitriev, Kokotushkin		Projection method Integral equation method	H-polarization E-polarization	Album, 4 1975 Album, 4 1975
Dmitriev, Tavartkiladze		Projection method Integral equation method	H-polarization E-polarization	Album, 5 1975 Album, 5 1975
Dmitriev, Tavartkiladze		Projection method Integral equation method	H-polarization E-polarization	Album, 5 1975 Album, 5 1975
Dmitriev, Tavartkiladze		Projection method	H-polarization	Album, 5 1975
Dmitriev, Tavartkiladze		Projection method	H-polarization	Album, 5 1975
Dmitriev, Tavartkiladze		Integral equation method	E-polarization	Album, 5 1975
Dmitriev, Tavartkiladze		Integral equation method	E-polarization	Album, 5 1975

a one-dimensional one or a three-dimensional problem to a two-dimensional one; 2. they open up ways for deriving analytical solutions and estimates.

Approximate boundary conditions for thin layers lie at the base of the asymptotic methods. These conditions are sufficiently exact if the layer thickness is far less than the electromagnetic wavelength, and if the layer conductivity shows slow horizontal variations.

The first asymptotic solution was due to PRICE [35] and SHEINMANN [39]. The Price—Sheinmann conditions were derived from the well-known ideas on the discontinuities of the electromagnetic field at the surface current and double layer. This method is widely used for describing the surface effects. It, however, disregards the finite thickness of the layer and therefore leads to large errors exaggerating the surface geomagnetic effects.

TIKHONOV and DMITRIEV [48] and DMITRIEV [13] suggested a modified method which improved the accuracy of simulation. This method, probably, is not widely known and we would like to discuss it in greater detail. As an example, let us consider a layer of constant thickness h and variable conductivity $\sigma(x, y)$. Expanding the horizontal components of the field into a Taylor series, and retaining only the first term, we can write

$$H_{x,y}^+ = H_{x,y}^- + h \frac{\partial H_{x,y}^-}{\partial z} \quad E_{x,y}^+ = E_{x,y}^- + h \frac{\partial E_{x,y}^-}{\partial z},$$

where the plus and minus signs denote the lower and upper sides of the layer. Using the Maxwell equations and substituting horizontal derivatives for the vertical derivatives, we obtain the following approximate boundary conditions:

$$\begin{aligned} H_x^+ - H_x^- &= E_y^- S + \frac{h}{i\omega\mu_0} \left(\frac{\partial^2 E_y^-}{\partial x^2} - \frac{\partial^2 E_x^-}{\partial x \partial y} \right) \\ H_y^+ - H_y^- &= -E_x^- S + \frac{h}{i\omega\mu_0} \left(\frac{\partial^2 E_y^-}{\partial x \partial y} - \frac{\partial^2 E_x^-}{\partial y^2} \right) \\ E_x^+ - E_x^- &= \frac{\partial}{\partial x} \left[T \left(\frac{\partial H_y^-}{\partial x} - \frac{\partial H_x^-}{\partial y} \right) \right] + i\omega\mu_0 h H_y^- \\ E_y^+ - E_y^- &= \frac{\partial}{\partial y} \left[T \left(\frac{\partial H_y^-}{\partial x} - \frac{\partial H_x^-}{\partial y} \right) \right] - i\omega\mu_0 h H_x^-, \end{aligned} \quad (12)$$

where

$$S = \sigma h \quad T = h/\sigma.$$

These conditions differ from those of PRICE and SHEINMAN in the terms proportional to h , consequently, they account for the finite thickness of the layer. By means of this method we can construct models consisting of several thin layers. The method can be readily extended to a variable thickness layer as well [20]. We shall illustrate the application of this method in the next section.

Developing this method, BERDICHEVSKIY and ZHDANOV [9] summed up the entire Taylor series, and derived the following approximate boundary conditions for the spectral densities of the magnetic field:

$$\begin{aligned} h_x^+ &= h_x^- \operatorname{ch}(h\sqrt{\alpha^2 + \beta^2}) + \frac{j_y^- - i\alpha h_z^-}{\sqrt{\alpha^2 + \beta^2}} \operatorname{sh}(h\sqrt{\alpha^2 + \beta^2}) \\ h_y^+ &= h_y^- \operatorname{ch}(h\sqrt{\alpha^2 + \beta^2}) - \frac{j_x^- + i\beta h_z^-}{\sqrt{\alpha^2 + \beta^2}} \operatorname{sh}(h\sqrt{\alpha^2 + \beta^2}) \\ h_z^+ &= h_z^- \operatorname{ch}(h\sqrt{\alpha^2 + \beta^2}) + i \frac{\alpha h_x^- + \beta h_y^-}{\sqrt{\alpha^2 + \beta^2}} \operatorname{sh}(h\sqrt{\alpha^2 + \beta^2}), \end{aligned} \quad (13)$$

where \mathbf{h}, \mathbf{j} are Fourier transforms of \mathbf{H} and $\mathbf{I} = \sigma \mathbf{E}$, α and β are the spatial frequencies at x and y respectively. These spectral conditions give satisfactory accuracy of modelling even under a rather rapid variation of σ [55].

With the help of the asymptotic methods we can quickly fill the gaps in the distortion theory associated with the three-dimensional surface effects. Recently, DEBABOV et al. [24] reported that they had elaborated a program for calculating the low-frequency electromagnetic field over near-surface structures of any shape.

3. Theoretical analysis of surface effects

Models of global effects connected with the action of oceans have been examined in the monograph by RIKITAKE [37] and in the review by ASHOUR [3]. Here we shall only deal with the local effects caused by the inhomogeneity of the sedimentary cover of continents. These effects can be classified into two groups: 1. galvanic effects generated by excess charges, 2. induction effects caused by excess currents.

Two-dimensional structures

We shall consider a two-dimensional model in which the upper layer contains a rectangular inhomogeneous inclusion of width $2d$ (Fig. 2) Here

$$\sigma_0 = 0 \quad \sigma_1(y) = \begin{cases} \sigma_1^e & |y| \geq d \\ \sigma_1^i(y) & |y| \leq d \end{cases}$$

$$\sigma_2 \ll \sigma_1(y) \quad h_2 \gg h_1 \quad \sigma_3 = \infty.$$

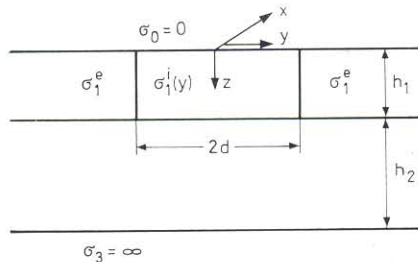


Fig. 2. Two-dimensional model with rectangular inclusion

The model is excited by a uniform plane wave. Following TIKHONOV and DMITRIEV [48], we shall make use of the asymptotic method based on the approximate boundary conditions (12).

Galvanic effects are exhibited in H -polarization. In this case, we have $\mathbf{E}\{0, E_y, E_z\}$, $\mathbf{H}\{H_x, 0, 0\}$. Applying the boundary conditions (12) to both the layers, we obtain a relationship between E_y and H_x at the earth surface:

$$T_2 \frac{d^2}{dy^2} [S_1(y) E_y(y)] - [1 - i\omega \mu_0 h_2 S_1(y)] E_y(y) = -i\omega \mu_0 (h_1 + h_2) H_x(y), \quad (14)$$

where

$$S_1(y) = h_1 \sigma_1(y) \quad T_2 = h_2 / \sigma_2.$$

In studying the H -polarized field, we can put $H_x = H_0 = \text{const}$ on the earth surface, where H_0 is the doubled external field. Thus Eq. (14) is converted into a differential equation for E_y . It is more convenient to reduce this equation to an integral equation:

$$E_y(y) = -\frac{S_1^e}{S_1(y)} Z^N H_0 + \frac{\tau}{2S_1(y) \sqrt{1 - i\omega \mu_0 h_2 S_1^e}} \int_{-d}^{+d} E_y(y') [S_1(y') - S_1^e] e^{-\tau \sqrt{1 - i\omega \mu_0 h_2 S_1^e} |y' - y|} dy', \quad (15)$$

where Z^N is the normal impedance, i.e. the impedance in the absence of inhomogeneity:

$$Z^N = \frac{i\omega \mu_0 (h_1 + h_2)}{i\omega \mu_0 h_2 S_1^e - 1}$$

and τ is the galvanic parameter which specifies the degree of current penetration into the resistive layer σ_2 :

$$\tau = \frac{1}{\sqrt{T_2 S_1^e}} = \sqrt{\frac{\sigma_2}{h_1 h_2 \sigma_1^e}}.$$

There are no anomalies of H_x in this model, whereas the anomalies of E_y depend appreciably on τ . All necessary estimates can be made using the integral equation (15).

If $\tau \rightarrow 0$, the contribution of the integral term to E_y is negligibly small. Therefore

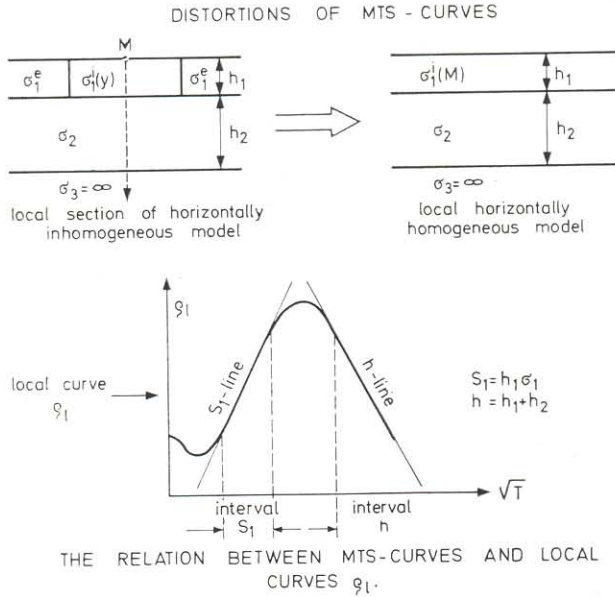
$$E_y(y) = -\frac{S_1^e}{S_1(y)} Z^N H_0, \quad (16)$$

that holds true if

$$\frac{\max |S_1(y) - S_1^e|}{\min S_1(y)} (1 - e^{-\tau d}) < 0.1. \quad (17)$$

This means the current flows over a nonuniform layer σ_1 without penetrating into the layer σ_2 .

Table III.



frequency interval field polarization	interval S	interval h	formal interpretation
H-polarization $\varphi^+(y) =$	$\varphi_1(y)$ The ascending branch of φ^+ is <u>not distorted</u>	$\left(\frac{S_1^e}{S_1(y)}\right)^2 \varphi_1(y)$ The descending branch of φ^+ is distorted by <u>galvanic S-effect</u>	false structures of conducting basement relief may arise
E-polarization $\varphi^-(y) =$	$\left(\frac{S_1(y)}{S_1(y, \omega)}\right)^2 \varphi_1(y)$ The ascending branch of φ^- is distorted by <u>induction effect</u>	$\varphi_1(y)$ The descending branch of φ^- is <u>not distorted</u>	false conducting layers may arise

By virtue of (16) we have

$$E_y(y) = \frac{S_1^e}{S_1(y)} E_y^N, \tag{18}$$

where E_y^N is the normal electrical field. Hence

$$\frac{E_y(y) - E_y^N}{E_y^N} = \frac{S_1^e}{S_1(y)} - 1. \tag{19}$$

It is clear that the anomalies of E_y are local and do not depend on the frequency. These properties of the electrical field are characteristic of galvanic effects observed in the two-dimensional case.

Now we shall examine the transversal impedance:

$$Z^\perp(y) = -\frac{E_y(y)}{H_0} = \frac{S_1^e}{S_1(y)} Z^N. \quad (20)$$

For sake of comparison we shall introduce the local impedance (Table III):

$$Z_l(y) = \frac{i\omega\mu_0(h_1 + h_2)}{i\omega\mu_0 h_2 S_1(y) - 1}, \quad (21)$$

i.e. the impedance of the horizontally uniform model formed by extrapolation of the local section of the observation site. The transversal curve $\varrho^\perp = |Z^\perp|^2/\omega\mu_0$ is distorted if it differs from the local curve $\varrho_l = |Z_l|^2/\omega\mu_0$.

In our model the local MTS curves are composed of an ascending branch, which reflects the resistive layer σ_2 , and a descending branch due to the conducting basement σ_3 . The frequency intervals of ascending and descending branches are called the interval S_1 and interval h . The boundaries of these intervals are found from the conditions:

$$\left(\frac{h_2}{h_1}\right)^2 > [\omega\mu_0 h_2 S_1(y)]^2 \gg 1 \quad \text{interval } S_1$$

$$[\omega\mu_0 h_2 S_1(y)]^2 \ll 1 \quad \text{interval } h. \quad (22)$$

Thus, we have

$$|Z_l(y)| = \begin{cases} \frac{1}{S_1(y)} & \text{in interval } S_1 \\ \omega\mu_0(h_1 + h_2) & \text{in interval } h. \end{cases} \quad (23)$$

We shall now compare Z^\perp with Z_l . We have $Z^\perp = Z_l$ outside the inclusion. Here the MTS curves are free of distortions: $\varrho^\perp = \varrho_l$. Over the inclusions, however, we find an entirely different picture. Here

$$|Z^\perp(y)| = \begin{cases} |Z_l(y)| & \text{in interval } S_1 \\ \frac{S_1^e}{S_1(y)} |Z_l(y)| & \text{in interval } h. \end{cases} \quad (24)$$

Consequently,

$$\varrho^\perp(y) = \begin{cases} \varrho_l(y) & \text{in interval } S_1 \\ \left[\frac{S_1^e}{S_1(y)}\right]^2 \varrho_l(y) & \text{in interval } h. \end{cases} \quad (25)$$

In interval S_1 the impedance Z^\perp coincides with Z_i in modulus. Thus, we have the same relationship as in a horizontally uniform model. In this case $q^\perp = q_i$, i.e. the ascending branches of transversal MTS curves are not distorted, and they define the true distribution of S_1 .

In interval h the impedance Z^\perp differs from Z_i by a factor $S_1^e/S_1(y)$, i.e. it depends on $S_1(y)$, though there is no such relationship in the horizontally

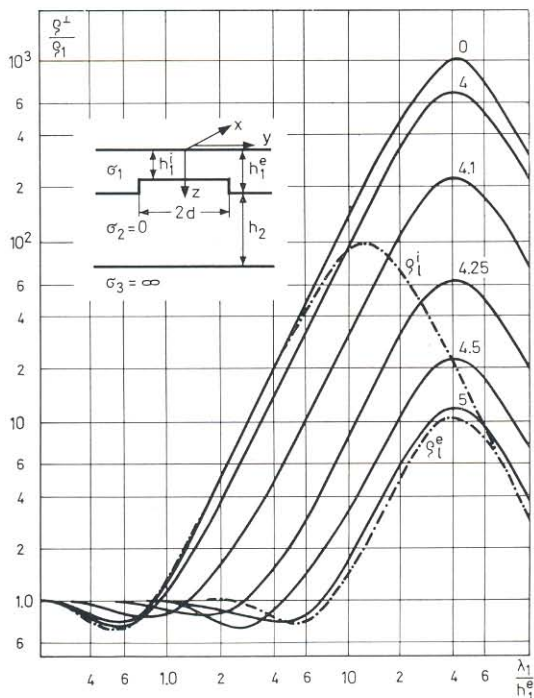


Fig. 3. Transversal MTS curves in horst model; $h_1^i/h_1^e = 0.1$, $h_2^e/h_1^e = 20$, $d/h_1^e = 4$; curves q^\perp are digitized by $|y|/h_1^e$; q_i^e , q_i^e are local curves

uniform model. We shall call this galvanic effect the *S-effect*. It is a consequence of the fact that the resistive layer σ_2 hampers the flow of current from layer σ_1 to layer σ_3 . The *S-effect* distorts the descending branches of transversal MTS curves $q^\perp \neq q_i$. They shift upward if $S_1(y) < S_1^e$, and downward if $S_1(y) > S_1^e$. A formal interpretation of such curves gives a false structure to the relief of the conducting basement. False depressions correspond to the minima of S_1 , false elevations to the maxima of S_1 .

Figure 3 shows the transversal MTS curves obtained in a horst model [17]. The *S-effect* is quite obvious here. The descending branches of curves q^\perp are shifted upward relative to the descending branches of the local curves q_i^e and q_i^e calculated for a horizontally uniform model with upper layer thickness h_1^i

and h_1^e , respectively. Formal interpretation of the ϱ^\perp curves gives a false depression in the relief of the conducting basement.

The factor $S_1^e/S_1(y)$ expresses maximum S -effect characteristic of small τ . For large τ , the excess current penetrates into the layer σ_2 , and the S -effect is considerably weakened. If

$$\max \left| \frac{dS_1(y)}{dy} \right| < 0.1 \min \tau \min S_1(y), \quad (26)$$

where

$$\min \tau = \frac{1}{\sqrt{T_2 \max S_1(y)}},$$

there is almost no S -effect ($\varrho^\perp \approx \varrho_l$).

It is worth while to give some examples of cases which satisfy conditions (17) and (26)

Example 1. The total conductivity of sedimentary cover varies from 500 mhos at the elevation of the crystalline basement to 1000 mhos at its slopes. The width of elevation is 30 km. The Earth's crust and the upper mantle have an average conductivity of 10^{-4} mho/m. A good conducting matter is at a depth of 200 km. Thus, we have $\max S_1 = 1000$ mhos, $\min S_1 = 500$ mhos, $\sigma_2 = 10^{-4}$ mho/m, $h_2 = 2 \cdot 10^5$ m, $d = 1.5 \cdot 10^4$ m. These data satisfy the conditions (17). Consequently, maximum S -effect is observed.

Example 2. The total conductivity of the sedimentary cover varies from 300 mhos to 500 mhos. Maximum gradient of S_1 is 0.3 mho/km. The sedimentary cover is insulated from the conducting matter of the Earth's crust by a 10 km thick layer. The mean conductivity of this layer is 10^{-3} mho/m. Thus, we have $\max S_1 = 500$ mhos, $\min S_1 = 300$ mhos, $\max |dS_1/dy| = 3 \cdot 10^{-4}$ mho/m, $\sigma_2 = 10^{-3}$ mho/m, $h_2 = 10^4$ m. It is easy to verify that these data satisfy condition (26). Consequently, there is almost no S -effect.

Example 1 is typical of many regions of the globe, whereas example 2 illustrates an extraordinary situation. We should note here that the MTS curves are almost always distorted by the S -effect.

Induction effects are exhibited in E -polarization. In this case we have $E\{E_x, 0, 0\}$, $H\{0, H_y, H_z\}$. With the help of the approximate conditions (12), we obtain a relationship between E_x and H_y on the earth surface:

$$h_1 h_2 \frac{dE_x(y)}{dy^2} - [1 - i\omega \mu_0 h_2 S_1(y)] E_x(y) = i\omega \mu_0 (h_1 + h_2) H_y(y), \quad (27)$$

where

$$H_y(y) = \frac{1}{i\omega \mu_0} \left. \frac{\partial E_x(y, z)}{\partial z} \right|_{z=0}.$$

This relationship can be regarded as the boundary condition of the problem for E_x in air. On applying the Green theorem to the region $z \leq 0$, the problem is reduced to an integral equation for E_x at $z = 0$:

$$E_x(y) = E_x^N + \frac{i\omega\mu_0 h_2}{h_1 + h_2} \int_{-d}^{+d} E_x(y') [S_1(y') - S_1^e] G(y, y') dy', \quad (28)$$

where E_x^N is the normal electrical field, and G is the Green function:

$$G(y, y') = \frac{h_1 + h_2}{\pi} \int_0^\infty \frac{\cos t(y - y') dt}{h_1 h_2 t^2 + (h_1 + h_2)t + (1 - i\omega\mu_0 h_2 S_1^e)}, \quad (29)$$

which describes the induction influence of excess current flowing in the near-surface layer.

The Green function with the pre-integral factor plays the role of a spatial filter whose selectivity depends on frequency (Fig. 4). The higher the frequency, the narrower the filter pass-band, and hence the more expressed is the locality of E_x . If at the beginning of the interval S_1 we observe an electrical field reflecting an average S_1 in the vicinity of the observation point, then the remote portions of the near-surface layer begin to affect with decreasing frequency. The lateral influence of zones with higher S_1 diminishes the value of E_x . The integral equation (28) is an effective tool for estimating the long-range action of inhomogeneity. We shall confine ourselves to an estimation for the interval S_1 . Outside the non-uniform inclusion its influence can be disregarded if

$$\frac{1}{2\pi^3} \left(\frac{\lambda_1^e}{r} \right)^2 \frac{d}{h_1} \frac{1}{1 + 2d/r} \frac{\max |S_1(y) - S_1^e|}{\min S_1(y)} < 0.1 \quad (30)$$

where $r = |y| - d$ is the distance up to the edge of inclusion, λ_1^e is the wavelength in the uniform part of the near-surface layer:

$$\lambda_1^e = \frac{2\pi\sqrt{2}}{\sqrt{\omega\mu_0\sigma_1^e}} = \frac{2\pi\sqrt{2h_1}}{\sqrt{\omega\mu_0 S_1^e}}.$$

When $\omega \rightarrow 0$, the contribution of the integral term into E_x becomes negligibly small, and hence we have $E_x \rightarrow E_x^N$ at all points of the earth surface. Thus, the anomalies of E_x develop in the interval S_1 , and they vanish at the end of the interval S_1 or in passing to the interval h depending on the width of the inhomogeneity.

Now we shall turn our attention to an analysis of magnetic anomalies. From the relationships (27) and (28) we can easily derive formulas

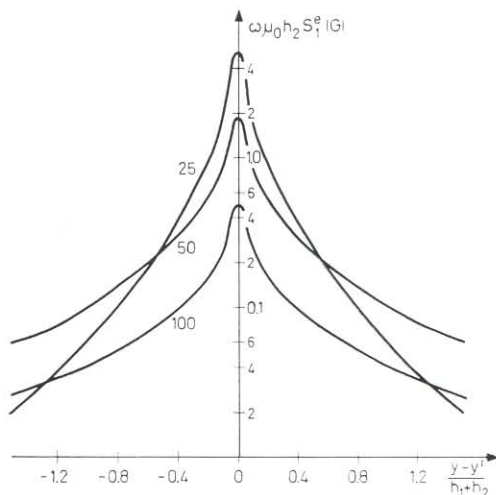


Fig. 4. Green function; $h_2/h_1 = 49$; curves are digitized by λ_1^e/h_1 , where λ_1^e is the wavelength in the uniform part of the near-surface layer

for H_y and H_z on the earth surface:

$$H_y(y) = H_y^N + \frac{h_2}{h_1 + h_2} \int_{-d}^{+d} E_x(y') [S_1(y') - S_1^e] K(y, y') dy' \quad (31)$$

$$H_z(y) = \frac{h_2}{h_1 + h_2} \int_{-d}^{+d} \frac{\partial}{\partial y'} \{E_x(y') [S_1(y') - S_1^e]\} G(y, y') dy', \quad (32)$$

where H_y^N is the normal magnetic field, K is a function obtained by differentiating the Green function:

$$K(y, y') = \frac{h_1 + h_2}{\pi} \int_0^{\infty} \frac{t \cos t(y - y') dt}{h_1 h_2 t^2 + (h_1 + h_2)t + (1 - i\omega \mu_0 h_2 S_1^e)} \quad (33)$$

The function K , as the Green function, acts as a spatial filter. The higher the frequency, the narrower the pass-band of this filter. At the beginning of the interval S_1 , the contribution of the integral term to H_y is rather small and the anomalies of H_y are weak. But they become stronger with decreasing frequency, as the filter pass band increases, and the contribution of the integral term grows (influence of excess current increases). The degree of field locality in this case decreases. Anomalies of H_y reach maximum at the end of the interval S_1 . On passing on to interval h , the anomalies of H_y rapidly decrease and vanish because here E_x is proportional to ω and the contribution of the integral term is negligibly small. The same regularities are characteristic of the anomalies of H_z caused by the asymmetry of excess currents.

Thus, the anomalies of E_x , H_y , H_z are integral and depend on the frequency. They vanish when $\omega \rightarrow 0$. These properties are characteristic of induction effects.

For $d < h_2$, we obtain the following estimates for the anomalies of E_x , H_y , H_z :

$$\begin{aligned}
 \left| \frac{E_x(y) - E_x^N}{E_x^N} \right| &< \begin{cases} \frac{8\pi}{\left(\frac{\lambda_1^e}{h_1}\right)^2} \frac{d}{h_1} \max \left| \frac{S_1(y)}{S_1^e} - 1 \right| \ln \left[1 + \frac{1}{32\pi^4} \left(\frac{\lambda_1^e}{\sqrt{h, d}} \right)^4 \right] & \text{in interval } S_1 \\ \frac{8\pi}{\left(\frac{\lambda_1^e}{h_1}\right)^2} \frac{d}{h_1} \max \left| \frac{S_1(y)}{S_1^e} - 1 \right| \ln \left[1 + 2 \left(\frac{h_2}{d} \right)^2 \right] & \text{in interval } h \end{cases} \\
 \left| \frac{H_y(y) - H_y^N}{H_y^N} \right| &< \begin{cases} \frac{4}{\pi} \max \left| \frac{S_1(y)}{S_1^e} - 1 \right| \ln \frac{1}{2\pi\sqrt{2}} \frac{\lambda_1^e}{h_1} & \text{in interval } S_1 \\ \frac{16\pi}{\left(\frac{\lambda_1^e}{h_1}\right)^2} \frac{h_2}{h_1} \max \left| \frac{S_1(y)}{S_1^e} - 1 \right| \ln \frac{h_2}{h_1} & \text{in interval } h \end{cases} \quad (34) \\
 \left| \frac{H_z(y)}{H_y^N} \right| &< \begin{cases} \frac{1}{\pi} \frac{h_2}{S_1^e} \max \left| \frac{d S_1(y)}{dy} \right| \ln \left[1 + \frac{1}{32\pi^4} \left(\frac{\lambda_1^e}{\sqrt{h, d}} \right)^4 \right] & \text{in interval } S_1 \\ \frac{8\pi}{\left(\frac{\lambda_1^e}{h_1}\right)^2} \frac{h_2^2}{h_1 S_1^e} \max \left| \frac{d S_1(y)}{dy} \right| \ln \left[1 + 2 \left(\frac{1}{\pi} \frac{h_2}{S_2^e} \right)^2 \right] & \text{in interval } h. \end{cases}
 \end{aligned}$$

We shall give an example of the estimates of the E_x , H_y , H_z anomalies. Let the total conductivity of sedimentary cover vary from 1500 mhos at the centre of a depression to 100 mhos at its edges. The depression width is 400 km. The average thickness of sedimentary cover is 3 km. Maximum gradient of S_1 is 10 mho/km. Conducting matter lies at a depth of 300 km. We shall estimate the anomalies of diurnal variation. We have $h_1 = 3 \cdot 10^3$ m, $h_2 = 3 \cdot 10^5$ m, $d = 2 \cdot 10^5$ m, $S_1^e = 100$ mhos, $\max S_1 = 1500$ mhos, $\max |dS_1/dy| = 10^{-2}$ mho/m, $\omega = 2\pi \cdot 10^{-5}$ sec $^{-1}$. Thus, $\omega\mu_0 h_2 \max S_1 = 0.04$, i.e. the diurnal variation belongs everywhere to the interval h . By virtue of (34), we have

$$\left| \frac{E_x(y) - E_x^N}{E_x^N} \right| < 10^{-2} \quad \left| \frac{H_y(y) - H_y^N}{H_y^N} \right| < 10^{-1} \quad \left| \frac{H_z(y)}{H_y^N} \right| < 4 \cdot 10^{-2}.$$

Therefore, the diurnal variation is almost not distorted.

Let us now show an exact calculation which illustrates the specific features of induction effects. Figure 5 represents the amplitude and phase curves of E_x , H_y , H_z obtained in a model with rectangular inclusion of higher con-

ductivity $\sigma_1^i = \text{const}$ [17]. The amplitude of E_x has a minimum over the inclusion. In the interval S_1 the maxima of $|H_y|$ are confined to the edges of the inclusion. They are explained by the concentration of excess current near the contacts, i.e. by the horizontal skin-effect. On passing over to the interval h , the lateral maxima of $|H_y|$ vanish and a central maximum of $|H_y|$ appears. Maxima of amplitude of H_z are observed over the inclusion edges where the asymmetry of excess currents is most pronounced. The anomaly of E_x decays and ultimately diminishes with decreasing frequency, whereas the anomalies of H_y , H_z increase in the interval S_1 and diminish in passing on to interval h where the phase difference between H_z and H_y^N approaches a value of $-\pi/2$.

Now we shall turn our attention once again to the relationships (28) and (31), and determine the longitudinal impedance $Z^{\parallel} = E_x/H_y$.

Recalling the properties of E_x , H_y we can take

$$|Z^{\parallel}(y)| = \begin{cases} 1 & \text{in interval } S_1 \\ \tilde{S}_1(y, \omega) & \\ \omega\mu_0(h_1+h_2) & \text{in interval } h, \end{cases} \quad (35)$$

where \tilde{S}_1 is the average total conductivity of the near-surface layer at a frequency ω . The lower the frequency, the wider the averaged zone. Thus, we have

$$|Z^{\parallel}(y)| = \begin{cases} \frac{S_1(y)}{\tilde{S}_1(y, \omega)} |Z_l(y)| & \text{in interval } S_1 \\ |Z_l(y)| & \text{in interval } h \end{cases} \quad (36)$$

$$\varrho^{\parallel}(y) = \begin{cases} \left[\frac{S_1(y)}{\tilde{S}_1(y, \omega)} \right]^2 \varrho_l(y) & \text{in interval } S_1 \\ \varrho_l(y) & \text{in interval } h. \end{cases} \quad (37)$$

In interval S_1 the impedance Z^{\parallel} differs from Z_l by a factor $S_1(y)/\tilde{S}_1(y, \omega)$, i.e. it depends on the average total conductivity of the near-surface layer which is a function of frequency. This integral dependence is responsible for the deformation of the ascending branches of the ϱ^{\parallel} -curves: $\varrho^{\parallel} \neq \varrho_l$. The deviations of ϱ^{\parallel} from ϱ_l reflect the horizontal variations of $S_1(y)$ in a smooth form. The lateral influence of maxima (minima) of S_1 decrease (increase) the

value of ϱ^{\parallel} . Due to the induction effect, the MTS sounding develops not only in a vertical direction, but also in a horizontal direction.

In interval h , the impedance Z^{\parallel} coincides with Z_1 in modulus. Therefore, we have $\varrho^{\parallel} = \varrho_1$, i.e. the descending branches of longitudinal MTS curves are not distorted. The relationship typical of horizontally uniform layer in this case is restored.

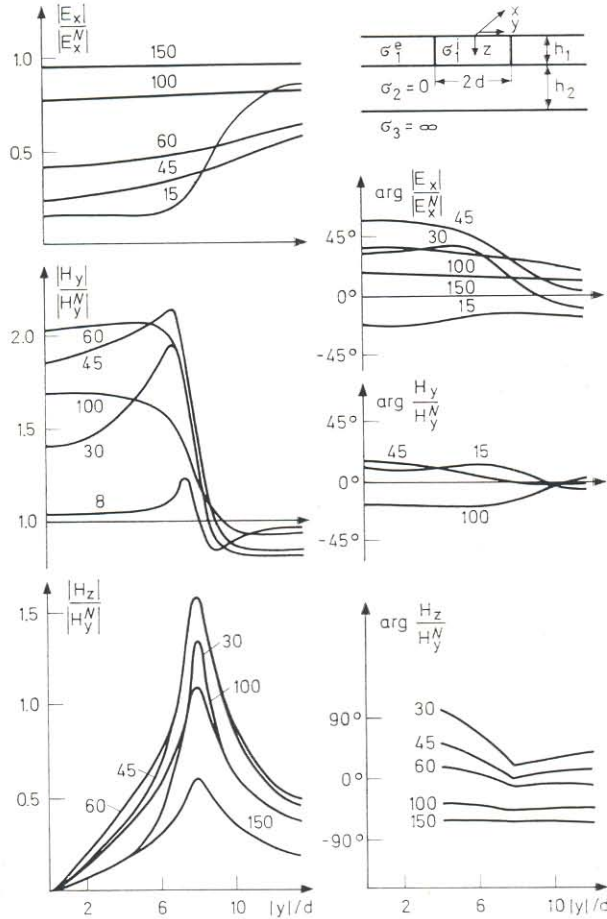


Fig. 5. Surface electromagnetic anomalies in a model with rectangular inclusion; $h_2/h_1 = 21$, $d/h_1 = 8$, $\sigma_1^e/\sigma_2^e = 16$; curves are digitized by λ^e/h_1

Formal interpretation of longitudinal MTS curves allows determining the true depth of the conducting basement σ_3 ; nonetheless, it may give false ideas as regards the conductivity of the intermediate layer σ_2 .

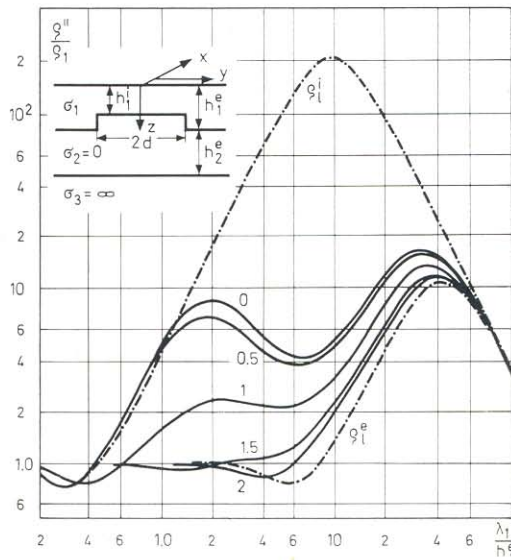


Fig. 6. Longitudinal MTS curves in horst model; $h_1^i/h_1^e = 0.05$, $h_2^e/h_1^e = 20$, $d/h_1^e = 1$; curves $\rho_1^||$ are digitized by $|y|/h_1^e$; ρ_1^i , ρ_1^e are local curves

Figure 6 shows the longitudinal curves $\rho_1^||$ in a horst model [16]. They are good illustrations of the induction effect. The curves $\rho_1^||$ obtained over the horst have a deep minimum which reflects the lateral influence of a conducting zone bordering the horst. Formal interpretation of such curves creates a false conducting layer beneath the horst. The curves $\rho_1^||$ obtained at a distance from the horst are slightly distorted.

All these results are generalized in Table III.

Three-dimensional structures

So far, only a limited number of problems have been solved. This part of the distortion theory needs further development. All those effects already discussed are also observed in three-dimensional situations, but they are less strongly expressed. Moreover, several new galvanic effects appear as results of field curvature. These effects can be reduced to flow-around (the current flows around resisting structures) and to concentration (the current concentrates in conducting structures). MTS curves obtained in a model with elliptical inclusion are shown in Figs 7 and 8 [10]. The anomalous field was calculated by the formulas for direct current. If $\sigma_1^i < \sigma_1^e$, the flow-around

effect is quite evident. Near the inclusion the tangential component of E increases, whereas the normal component decreases. Therefore, the curve ϱ_{xy} is shifted upward, and the curve ϱ_{yx} downward. Over the inclusion both curves are shifted to the right. For $\sigma_1^i > \sigma_1^e$, concentration effect is exhibited. Near

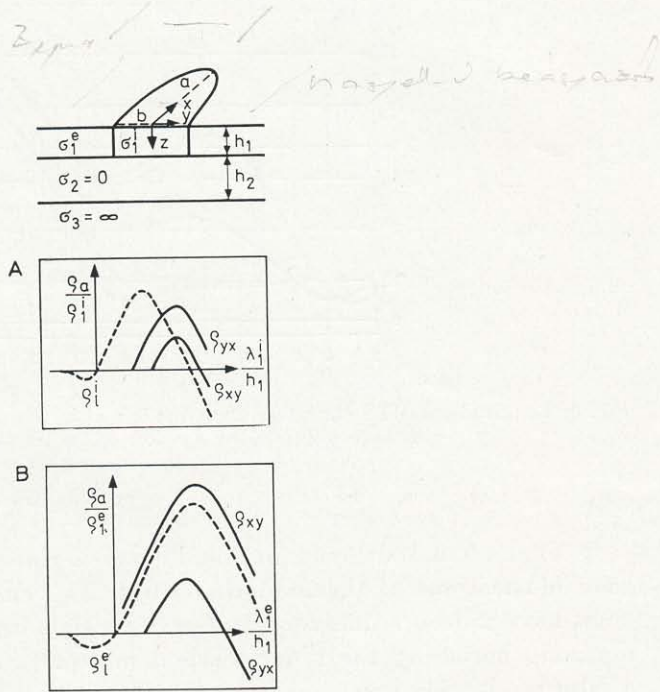


Fig. 7. MTS curves in a three-dimensional model with elliptical inclusion; $a/b = 2$, $\sigma_1^i/\sigma_1^e = 1/16$, $h_2/h_1 = 20$; ϱ_i^i, ϱ_i^e are local curves; A — over the inclusion, B — outside the inclusion ($x/b = 0, |y|/b = 1.5$)

the inclusion the curve ϱ_{xy} is shifted downward, while the curve ϱ_{yx} upward. Over the inclusion both curves are shifted to the left. This rough model reveals the most important characteristics of flow-around and concentration effects: a) both effects are observed in intervals S_1 and interval h as well, b) they do not vanish with decreasing frequency, c) they are attenuated at a distance comparable with the major axis of the structure, d) formal interpretation of MTS-curves distorted by flow-around and concentration effects gives rise to false conducting layers and creates a false relief of the conducting basement, e) in case of isometric structures, better results are given by the interpretation of average MTS curves constructed, using one of the impedance tensor invari-

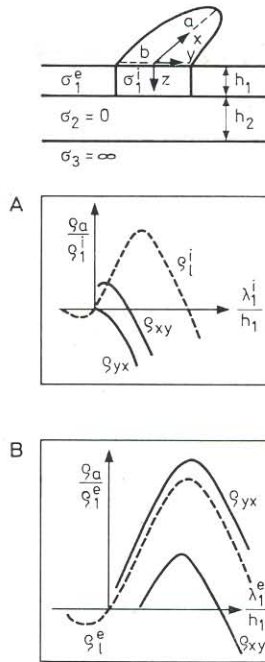


Fig. 8. MTS curves in a three-dimensional model with elliptical inclusion; $a/b = 2$, $\sigma_1^i/\sigma_1^e = 16$, $h_2/h_1 = 20$; ϱ_1^i, ϱ_1^e are local curves; A — over the inclusion, B — outside the inclusion ($x/b = 0$, $|y|/b = 1.5$)

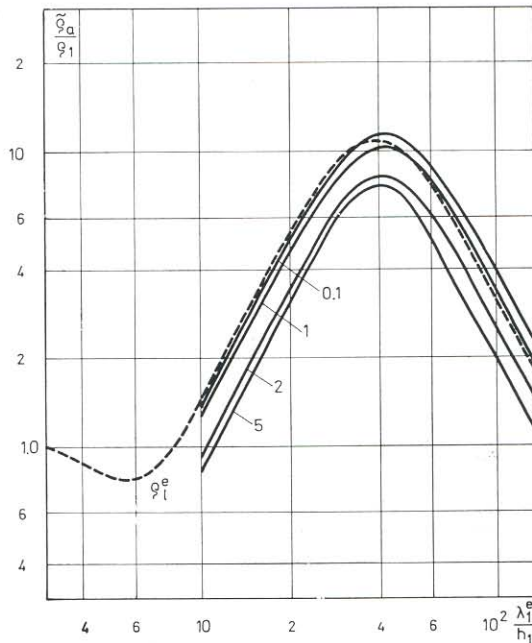


Fig. 9. Average MTS curves in a three-dimensional model with elliptical inclusion; curves have been calculated with the invariant $1/2(Z_{xy} - Z_{yx})$; $\sigma_1^i/\sigma_1^e = 16, 1/16$; observation site is outside the inclusion ($x/b = 0, |y|/b = 1.5$); curves are digitized by a/b ; ϱ_1^e is local curve

ants (Fig. 9). Analysis of the model shows that the structure could be looked upon as a quasi-two-dimensional one if its major axis is $10|S_1^i/S_1^e - 1|$ times greater than its minor axis. Magnetic anomalies in a model with round inclusion have been investigated by ASHOUR and CHAPMAN [2]. It should be mentioned that in a model with arbitrary inhomogeneity of the near-surface layer the magnetic anomalies are less than in the two-dimensional situation obtained by infinite elongation of structures and thus they can be evaluated with the help of the formula (34). In passing on to interval h these anomalies decrease and vanish.

Influence of the spatial non-uniformity of the external field

Up to now, we have tacitly supposed the near-surface structures to be local and not to extend out of the region where the external field could be approximated by a plane wave. But if the structures are thousands of kilometres long, the non-uniformity of the external field gets appreciable and the TIKHONOV—CAGNIARD model might disagree with the experimental results. An excellent example of such a disagreement is the edge effect observed in elongated depressions [10]. The depression serves as a channel for the current, and the low frequency electrical field is polarized along its axis, reducing the transversal impedance. The curves ϱ^\perp are deformed and shifted downward. This effect is enhanced near the edges of the depression. The first theoretical model of edge effect was proposed by OBUKHOV and SAFONOV [32].

*

Detailed analysis of surface effects is given in [26]. The influence of earth surface relief is reviewed by DMITRIEV and TAVARTKILADZE [22].

4. Diagnostics of surface effects

The more exhaustive the information on the structure of sedimentary cover and the more complete the experimental data, the more reliable is the solution of this problem.

In magnetotelluric sounding we generally compare the transversal and longitudinal curves ϱ_a , reveal the contradictions in their formal interpretation, correlate the parameters obtained, investigate the dependence between the characteristic points of MTS curves and the distance up to the inhomogeneities, study the magnetic anomalies, make use of simplified estimates, and simulate complicated situations. Such an analytical procedure gives a sufficiently complete system of criteria for detecting the surface effects [6, 10].

If the MTS data show that the total conductivity of the sedimentary cover and the depth of the deep conducting layer are in inverse dependence,

we have every ground to suppose that this is due to the *S*-effect (Fig. 10). Another criterion for the *S*-effect is the weak dependence between the abscissas of maxima of the MTS curves and the depths of the conducting layer.

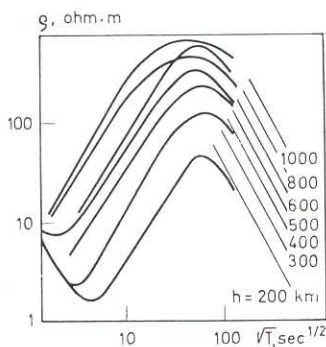


Fig. 10. These MTS curves obtained in the northwestern part of the Russian platform are in all probability distorted by *S*-effect

A false conducting layer, caused by the induction effect, is recognized with the help of simplified estimates and trial models and by the following visual criteria: 1. minima or inflexions of longitudinal curves vanish rapidly as the distance from the depression increases, 2. there are no minima or inflexions on the transversal curves. If the minima or the inflexions of longitudinal MTS curves remain on passing over to the central part of the depression, it might serve as an evidence in favour of the existence of a conducting layer.

An instructive theoretical example is shown in Fig. 11. The transversal and longitudinal MTS curves obtained over the two-dimensional horst are represented. The curve ϱ^{\perp} is distorted by the *S*-effect: its descending branch is shifted upward. The curve ϱ^{\parallel} is distorted by the induction effect; it has a false minimum caused by the lateral influence of the zones bordering the horst. A comparison of the curves ϱ^{\perp} and ϱ^{\parallel} reveals both effects. By uniting the ascending branch of the curve ϱ^{\perp} with the descending branch of ϱ^{\parallel} , we can construct an undistorted sounding curve.

The transversal and longitudinal MTS curves along the profile intersecting the Precaucasian down-warp are shown in Fig. 12 [6]. Formal interpretation of these curves gives conflicting results. Judging by the curves ϱ^{\perp} , the Earth's crust contains a conducting layer subsiding towards the Caucasus. There is no such a layer in the section constructed from the curves ϱ^{\parallel} . Which result is real? On approaching the Caucasus, the field E polarizes along the

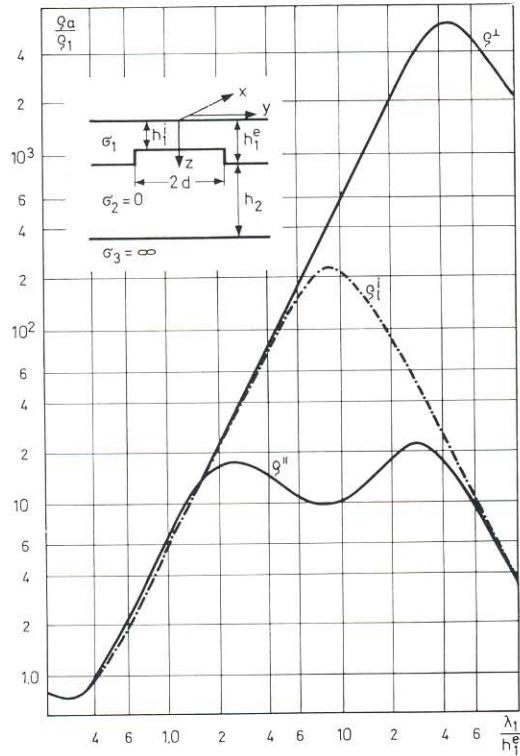


Fig. 11. MTS curves for the middle of horst; $h_1^i/h_1^e = 0.05$, $h_2^e/h_1^e = 20$, $d/h_1^e = 2$; q_1^i is the local curve

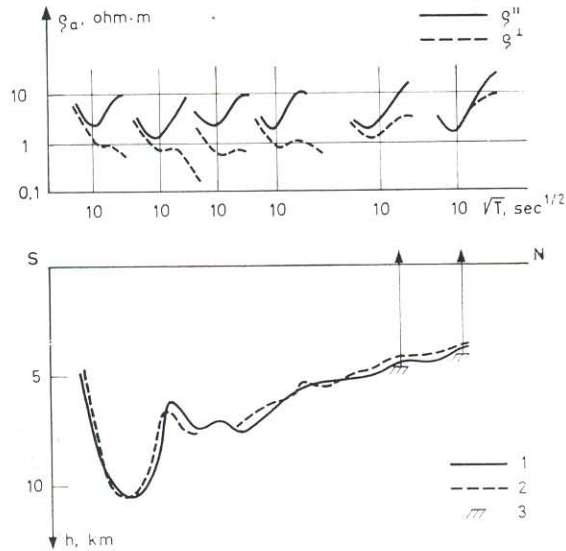


Fig. 12. Geophysical section along the profile crossing the Precaucasian down-warp; 1, 2, 3 — surface of the Paleozoic basement; 1 — according to curves q'' , 2 — according to seismics, 3 — according to drilling

down-warp, the ratio $\rho^{\parallel}/\rho^{\perp}$ increases, and the discrepancy between the curves ρ^{\parallel} and ρ^{\perp} begins at higher frequencies. These symptoms clearly indicate that the curves ρ^{\perp} are distorted by the edge effect which generates a false conducting layer. Thus, we can rely only on the longitudinal MTS curves which deny the existence of a conducting layer in the Earth's crust. It remains only to add that the depths of the Paleozoic basement determined with the help of the curves ρ^{\parallel} are in satisfactory agreement with seismic sounding data.

Diagnostics of magnetic anomalies is based a) on comparison with MTS curves, b) on a study of the phase relationship, c) on calculation of models which approximate the sedimentary cover.

5. Elimination of surface effects

Correction of magnetovariation data by model calculation is well-known [41, 38]. Therefore, we shall confine ourselves to a consideration of the methods based on the separation of weakly distorted situations and integral transformation of fields.

Separation of slightly distorted situations

This method is widely applied in magnetotelluric sounding in regions with quasi-two-dimensional structures of the sedimentary cover. The fact that longitudinal MTS curves are slightly distorted by the *S*-effect is used as a criterion for quasi-two-dimensionality. Under these conditions the low-frequency branches of the curves ρ^{\parallel} give sufficiently reliable information on the deep geoelectrical section. The transversal and longitudinal MTS curves obtained in the South-Caspian depression are shown in Fig. 13 [5]. The surface

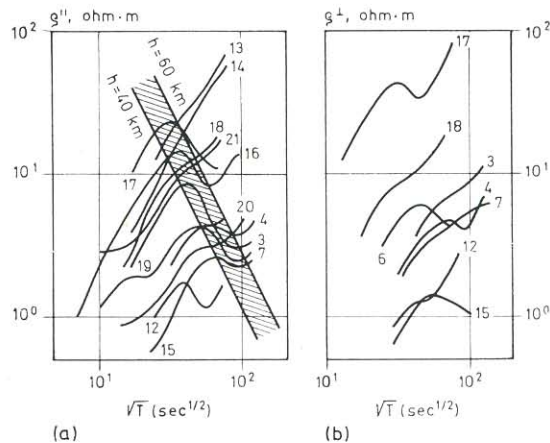


Fig. 13. MTS curves for the South Caspian depression; a — longitudinal curves, b — transversal curves

effects completely disorganize the curves ϱ^\perp , but the curves ϱ^\parallel at the same time are only slightly distorted. They are in good agreement and reflect the conducting layer at a depth from 40 to 60 km. Thus, the elimination of surface effects reduces to a selection of optimal polarization of the field.

In regions with three-dimensional structures of isometric form, we can diminish the influence of flow-around and concentration effects by using average MTS curves calculated with the help of one of the impedance tensor invariants. In this case, elimination of surface effects reduces to a selection of optimal representation for the sounding results.

Numerous examples of such an interpretation of MTS curves are given in the works of ANISHCHENKO, DUBROVSKIY, KOVTUN, KRASNOBAEVA, POSPEEV CHERNYAVSKIY published in [26].

In an analysis of the magnetic anomalies, the effect of surface inhomogeneities can be greatly diminished by choosing a sufficiently low-frequency field.

Integral transformation of the field

ZHDANOV and BERDICHEVSKIY proposed a method which permits one to derive electromagnetic sounding curves free from the effect of the near-surface layer [54, 55]. They used a plane model in which a non-uniform layer with known $\sigma_1(x, y)$ and h_1 lies on a uniformly layered medium. Calculations are divided into the following stages:

a) Fourier transformation of the field observed on the earth surface:

$$\begin{aligned} \mathbf{h}^- &= \int_{-\infty}^+ \int_{-\infty}^+ \mathbf{H}^- e^{i(\alpha x + \beta y)} dx dy \\ \mathbf{j}^- &= \int_{-\infty}^+ \int_{-\infty}^+ \sigma_1 \mathbf{E}^- e^{i(\alpha x + \beta y)} dx dy \end{aligned}$$

b) continuation of the Fourier transforms \mathbf{h}^- to the lower surface of the non-uniform layer with the help of the boundary conditions (13);

c) determination of the normal impedance Z^N by means of the continued Fourier transforms \mathbf{h}^+ :

$$Z^N = \frac{\omega \mu_0 h_z^+}{\alpha h_x^+ + \beta h_y^+} \quad (38)$$

The impedance Z^N characterizes a uniformly layered medium lying beneath the non-uniform layer. Such a normalization gives electromagnetic sounding curves which reflect the average distribution of deep electrical conductivity. This method is applicable if the structure of sedimentary cover is known. It calls for observations over a vast area and entails loss of local information.

Another problem, which could be solved by an integral field transformation, lies in dividing the magnetic anomalies into surface and deep parts. This method was suggested by BERDICHEVSKIY and ZHDANOV [8, 7]. Calculations can be conducted only if the structures of sedimentary cover and normal section of the Earth's crust and upper mantle are known. For sake of simplic-

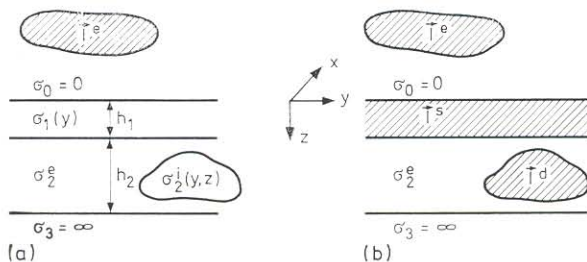


Fig. 14. Two-dimensional model with a near-surface and deep inhomogeneities *a*) and equivalent normal model *b*); areas containing excess currents are hatched

ity, we shall examine a two-dimensional model shown in Fig. 14a. The electrical conductivity of the near-surface layer varies with y . The intermediate layer contains a deep inhomogeneity Q . A perfect conductor lies beneath this layer. The model is excited by the external current I^e . The electromagnetic field has the components E_x , H_y , H_z and satisfies the equation:

$$\text{rot } \mathbf{H} = \begin{cases} \mathbf{I}^e & z \leq 0 \\ \sigma_1 \mathbf{E} = \mathbf{I}^s & 0 \leq z \leq h_1 \\ \sigma_2 \mathbf{E} = \sigma_2^e \mathbf{E} + \mathbf{I}^d & h_1 \leq z \leq h_1 + h_2 \end{cases}$$

$$\text{rot } \mathbf{E} = i\omega\mu_0 \mathbf{H} \quad z \leq h_1 + h_2,$$

where I^s is the current in the near-surface layer, I^d is the excess current in the inhomogeneity Q :

$$\mathbf{I}^s = \sigma_1 \mathbf{E} \quad \mathbf{I}^d = (\sigma_2 - \sigma_2^e) \mathbf{E}.$$

This model is equivalent to the normal model consisting of uniform layers σ_2^e , σ_3 and excited by current $I^e + I^s + I^d$ (Fig. 14b). Evidently, the magnetic field \mathbf{H} can be represented as the sum of \mathbf{H}^e , \mathbf{H}^s and \mathbf{H}^d excited in the normal model by the currents I^e , I^s and I^d respectively. The part \mathbf{H}^e can be identified as the normal field, the part \mathbf{H}^s contains the contribution of the near-surface layer, and the part \mathbf{H}^d describes the deep anomaly. Thus, the separation of the magnetic anomaly, and its division into surface and deep parts reduces to the determination of \mathbf{H}^s and \mathbf{H}^d .

The field \mathbf{H}^s can be found from the Fourier transform:

$$\bar{j}_x^- = \int_{-\infty}^{+\infty} I_x^s |_{z=0} e^{i\beta y} dy = \int_{-\infty}^{+\infty} \sigma_1 E_x^- e^{i\beta y} dy.$$

Indeed, by virtue of (13) and (38), we have

$$Z^N = \frac{\omega\mu_0 h_z^+}{\beta h_y^+} = \omega\mu_0 \frac{h_z^- \operatorname{ch}\beta h_1 + i h_y^- \operatorname{sh}\beta h_1}{\beta h_y^- \operatorname{ch}\beta h_1 - (j_x^- + i\beta h_z^-) \operatorname{sh}\beta h_1},$$

where Z^N is the impedance of normal model, h^+ and h^- are Fourier transforms of H^s at the lower ($z = h_1$) and upper ($z = 0$) surfaces of the layer σ_1 .

We express h^- in terms of the magnetic potential $ue^{|\beta|z}e^{-i\beta y}$:

$$h_y^- = i\beta u \quad h_z^- = -|\beta|u$$

Consequently,

$$Z^N = \frac{i\mu_0\omega}{|\beta|} \frac{e^{|\beta|h_1}}{e^{|\beta|h_1} + ij_x^- \frac{\operatorname{sh}\beta h_1}{u\beta^2}}. \quad (39)$$

On the other hand

$$Z^N = -\frac{i\omega\mu_0}{v_2} \operatorname{th}v_2 h_2 \quad v_2 = \sqrt{\beta^2 - i\omega\mu_0\sigma_2^e}. \quad (40)$$

Equating (39) and (40), and solving the equation obtained for u , we find

$$u = -i \frac{\operatorname{th}v_2 h_2}{2\beta} \frac{1 - e^{-2|\beta|h_1}}{v_2 + |\beta| \operatorname{th}v_2 h_2} J_x^-.$$

Hence

$$H_y^S = \frac{i}{2\pi} \int_{-\infty}^{+\infty} \beta u e^{-i\beta y} d\beta \quad H_z^S = -\frac{1}{2\pi} \int_{-\infty}^{+\infty} |\beta| u e^{-i\beta y} d\beta. \quad (41)$$

The part H^d is determined in a similar way. The method can be extended to a many-layered model containing three-dimensional inhomogeneities. ZHDANOV and BILINSKIY analyzed the data for the profile intersecting the Carpathian anomaly, and established that the deep anomaly for $T = 1$ hour was at least twice greater than the surface anomaly.

Conclusions

In this review we have attempted to generalize the works dealing with the surface effects. We conclude by emphasizing that only a joint interpretation of magnetotelluric and magnetovariation data could give satisfactory solution of the surface effect problem which should be united with the inverse problem. It seems that in this way the magnetotelluric and magnetovariation methods would merge into a general method of deep electromagnetic studies based on the analysis of frequency and spatial characteristics of different field

components and impedances. A considerable progress has been made in this field but many questions still await further elucidation. The main task is to develop the technique for the interpretation of electromagnetic data in three-dimensional situations.

REFERENCES

1. ASHOUR, A. A.: The coastline effects on rapid geomagnetic variations. *Geoph. J. R. astr. Soc.*, 10 (1965), No. 2.
2. ASHOUR, A. A.—CHAPMEN, S.: The magnetic field of electric currents in an unbounded plane sheet, uniform except for a circular area of different uniform conductivity. *Geoph. J. R. astr. Soc.*, 10 (1965), No. 1.
3. ASHOUR, A. A.: Theoretical models for e.m. induction in the oceans. First Workshop of E. M. Induction in the Earth. Edinburgh, 1972.
4. BERDICHEVSKIY, M. N.—VANYAN, L. L.—DMITRIEV, V. I.: On the possibility of disregarding vertical currents in magnetotelluric sounding. *Fizika zemli*, 1971, No. 5.
5. BERDICHEVSKIY, M. N.—DUBROVSKIY, V. G.—LUBIMOVA, E. A.—MANAFLY, A. A.—NEPEOV, K. N.—FELDMAN, I. S.: Anomalies of electrical conductivity in the upper mantle and their geothermal interpretation. *Fizika zemli*, 1971, No. 7.
6. BERDICHEVSKIY, M. N.—DMITRIEV, V. I.—YAKOVLEV, I. A.—BUBNOV, V. P.—KONNOV, YU. K.—VARLAMOV, D. A.: Magnetotelluric sounding of horizontally non-uniform media. *Fizika zemli*, 1973, No. 1.
7. BERDICHEVSKIY, M. N.—ZHDANOV, M. S.—ZHDANOVA, O. N.: On the possibility of dividing anomalies of a variable geomagnetic field into surface and deep parts. *Geomagnetism i Aeronomiya*, 14 (1974), No. 1.
8. BERDICHEVSKIY, M. N.—ZHDANOV, M. S.: Analysis of anomalies of a variable geomagnetic field at the surface of a many-layered horizontally non-uniform Earth. *Geomagnetism i Aeronomiya*, 15 (1975), No. 2.
9. BERDICHEVSKIY, M. N.—ZHDANOV, M. S.: On the continuation of a variable geomagnetic field into horizontally non-uniform layers. In collected papers: "Geomagnitnie issledovaniya" (Geomagnetic investigations). *Sovetskoe Radio*, 1976, No. 15.
10. BERDICHEVSKIY, M. N.—DMITRIEV, V. I.: Basic principles of interpretation of magnetotelluric sounding curves. In the monograph "Geoelectric and Geothermal Studies. Akadémiai Kiadó, Budapest, 1976.
11. CAGNIARD, L.: Basic theory of the magnetotelluric method of geophysical prospecting. *Geophysics*, 18 (1953), No. 3.
12. DMITRIEV, V. I.—KOKOTUSHKIN, G. A.: A method for calculating the magnetotelluric field in a variable thickness layer. *Vychislitelnye metody i programirovanie*". *Trudy Vychislitel'nogo Tsentra*, Moscow State University, 1968, No. 10.
13. DMITRIEV, V. I.: Electromagnetic field in non-uniform media. *Trudy Vychislitel'nogo Tsentra*, Moscow State University, 1969.
14. DMITRIEV, V. I.: Magnetotelluric field in thin non-uniform layers. "Vychislitelnye metody i programirovanie". *Trudy Vychislitel'nogo Tsentra*, Moscow State University, 1969, No. 13.
15. DMITRIEV, V. I.—ZAKHAROV, E. V.: A method for solving the electrodynamic problems of non-uniform media. *Zhur. Vychis. Matem. i Matem. Fiz.*, Moscow, 1970, No. 6.
16. DMITRIEV, V. I.—KOKOTUSHKIN, G. A.: Album of magnetotelluric sounding curves for horizontally non-uniform media. *Trudy Vychislitel'nogo Tsentra*, Moscow State University, 1971, No. 1.
17. DMITRIEV, V. I.—ZAKHAROV, E. V.—KOKOTUSHKIN, G. A.: Album of magnetotelluric sounding curves for horizontally non-uniform media. *Trudy Vychislitel'nogo Tsentra*, Moscow State University, 1973, No. 2.
18. DMITRIEV, V. I.—ZAKHAROV, E. V.—KOKOTUSHKIN, G. A.: Method for calculating the magnetotelluric fields in horizontally non-uniform media. "Magnetotelluric field in non-uniform media". *Trudy Vychislitel'nogo Tsentra*, Moscow State University, 1973.
19. DMITRIEV, V. I.—ZAKHAROV, E. V.—KOKIN, YA. YA.: On the influence of the vertical magnetic component of a primary field on the field of a disk immersed in a layered medium. "Magnetotelluricheskie polya v neodnorodnykh sredakh". *Trudy Vychislitel'nogo Tsentra*, Moscow State University, 1973.

20. DMITRIEV, V. I.—KHRYCHKOVA, T. S.: On the influence of variations in the thickness of the surface layer on deep magnetotelluric sounding. "Vychislitelnye metody i programmirovaniye". *Trudy Vychislitel'nogo Tsentra*, Moscow State University, 1975.
21. DMITRIEV, V. I.: On the selection of mathematical models in magnetotelluric sounding problems. In the collected papers: "Elektromagnitnye zondirovaniya Zemli i Luny". Moscow State University Press, 1975.
22. DMITRIEV, V. I.—TAVARTKILADZE, SH. A.: An investigation of the influence of the earth surface relief on deep magnetotelluric sounding. In collected paper: "Elektromagnitnie zondirovaniya Zemli i Luny". Moscow University Press, 1975.
23. DOSSO, H. W.: Induction in laterally non-uniform conductors: scale model experiments. First Workshop of E. M. Induction in the Earth, Edinburgh, 1972.
24. DEBABOV, A. S.—BERDICHEVSKIY, M. N.—VANYAN, L. L.: Numerical simulation of distortions in magnetotelluric field created by arbitrary surface inhomogeneities. "Elektromagnitnie zondirovaniye", Trudy IV Simpoziuma po elektromagnitnim zondirovaniyam (Zvenigorod), Moscow State University, 1976.
25. ECKHARDT, D.—LARNER, K.—MADDEN, T.: Long-period magnetic fluctuations and mantle electrical conductivity estimates. *J. Geoph. Res.*, 68 (1963), No. 23.
26. Geoelectric and Geothermal studies in East Central Europe and Soviet Asia. KAPG Geophys. Monograph. Akadémiai Kiadó, Budapest 1976.
27. HOBBS, B. A.: Analytic solutions to global and local problems of electromagnetic induction in the Earth. Second Workshop on Electromagnetic Induction in the Earth, Ottawa, 1974.
28. JONES, F. W.: Induction in laterally non-uniform conductor: theory and numerical models. First Workshop on Electromagnetic Induction in the Earth, Edinburgh, 1972.
29. KUPRADZE, V. D.: Boundary value problems in oscillation theory and integral equations. *Izdat. tekh. i Teor. Lit.*, Moscow, 1950.
30. MADDEN, T.—NELSON, P.: A defence of Cagniard's magnetotelluric method. Project NR 371-401, MIT, Cambridge, Mass., 1964.
31. MÜLLER, G.: Grundproblem der mathematischen Theorie elektromagnetischer Schwingungen. Berlin, 1957.
32. OBUKHOV, G. G.—SAFONOV, A. S.: Influence of nonuniformity of the primary field on magnetotelluric sounding results. *Prikladnaya geofizika*, 1976. No. 84.
33. PARRY, J. R.: Integral equation formulations of scattering from two-dimensional inhomogeneities in a conductive Earth. Ph. D. thesis, Berkeley, University of California, 1969.
34. PRAUS, O.: Numerical and analogue modelling of induction effects in laterally non-uniform conductor. Second Workshop on Electromagnetic Induction in the Earth, Ottawa, 1974.
35. PRICE, A. T.: The induction of electric currents in non-uniform thin sheets and shells. *Quart. J. Mech. Appl. Math.*, 2, 1949.
36. PRICE, A. T.: The theory of magnetotelluric method when the source field is considered. *J. Geoph. Res.*, 67 (1962), No. 5.
37. RIKITAKE, T.: Electromagnetism and the Earth's Interior. Elsevier Publishing Co., London 1966.
38. ROKITYANSKIY, I. I.: An Investigation of the Anomalies of Electrical Conductivity by the Magnetotelluric Profiling Method. Naukova Dumka Publishing House, Kiev 1975.
39. SHEINMAN, S. M.: On the stabilization of electromagnetic fields in the Earth. *Prikladnaya geofizika, Gostoptekhizdat*, 1947, No. 3.
40. SCHMUCKER, U.: Interpretation of induction anomalies above nonuniform surface layers. *Geophysics*, 36 (1971), No. 1.
41. SCHMUCKER, U.: Anomalies of geomagnetic variations in the South-Western United States. University of California Press, 1970.
42. SRIVASTAVA, S. P.: Method of interpretation of magnetotelluric data when source field is considered. *J. Geoph. Res.*, 70 (1965), No. 4.
43. SWIFT, C. M.: A magnetotelluric investigation of an electrical conductivity anomaly in the South-Western US. Ph. D. Thesis, MIT, Mass., 1967.
44. TABOROVSKIY, L. A.: Integral equations for axisymmetric problems. *Geologiya i geofizika Novosibirsk*, 1972, No. 7.
45. TIKHONOV, A. N.: On the determination of electrical characteristics of deep layers of the Earth crust. *Doklady AN SSSR*, 73 (1950), No. 2.
46. TIKHONOV, A. N.—SHAKHSUVAROV, D. N.: On the possibility of using the impedance of natural electromagnetic field for studying the upper layer of the Earth. *Izv. AN SSSR, ser. geofizika*, 1956, No. 4.

47. ТИХОНОВ, А. Н.—БЕРДИЧЕВСКИЙ, М. Н.: An experience in the application of magnetotelluric methods for investigating the geological structure of sedimentary basins. *Fizika Zemli*, 1966, No. 2.
48. ТИХОНОВ, А. Н.—ДМИТРИЕВ, В. И.: Effect of surface inhomogeneities on deep magnetotelluric sounding. "Vychislitelnie metody i programmirovaniye", *Trudy Vychislitel'nogo Tsentra*, Moscow State University, 1969, No. 13.
49. WAIT, J. R.: On the relation between telluric currents and the Earth magnetic field. *Geoph.*, 19 (1954), No. 2.
50. WAIT, J. R.: Theory of magnetotelluric fields. *J. Res. NBS*, 66D, 1962.
51. WARD, S. H.—PEEPLES, W. J.—RYU, J.: Analysis of geoelectromagnetic data. "The Computer Methods in Geophysics", Academy Press, New York 1974.
52. WEIDELT, P.: Modellrechnungen zur elektromagnetischen Induktion in dreidimensionalen Strukturen. Kolloquium "Erdmagnetische Tiefensondierung" in Grafrath (Bayern, München, 1974).
53. YUKUTAKE, T.: Electromagnetic induction on a conductor bounded by an inclined surface. *Publications of the Dominion Observatory Ottawa*, 35 (1967), No. 8.
54. ZHDANOV, M. S.—БЕРДИЧЕВСКИЙ, М. Н.—ЗHDANOVA, O. N.: On the possibility of normalization of electromagnetic sounding curves. *Geomagnetism i Aeronomiya*, 14 (1974), No. 1.
55. ZHDANOV, M. S.—БЕРДИЧЕВСКИЙ, М. Н.—ЗHDANOVA, O. N.: On the surface anomalies of the variable electromagnetic field of the Earth. *Geomagnetism i Aeronomiya*, 15 (1975), No. 3.

ИСКАЖЕНИЕ МАГНИТНЫХ И ЭЛЕКТРИЧЕСКИХ ПОЛЕЙ, ВСЛЕДСТВИЕ БЛИЗКОПОВЕРХНОСТНЫХ ЛАТЕРАЛЬНЫХ НЕОДНОРОДНОСТЕЙ

М. Н. ВЕРДИЧЕВСКИЙ — В. И. ДМИТРИЕВ

РЕЗЮМЕ

Авторы рассматривают общую стратегию интерпретации с учетом поверхностных эффектов и излагают результаты, полученные в СССР. Статья состоит из пяти частей, посвященных следующим вопросам:

а) стратегии интерпретации магнитотеллурических и магнитовариационных измерений, б) моделированию поверхностных эффектов, в) теоретическому анализу этих эффектов, г) их диагностике, д) устранению искажений поля.